




## RESEARCH ARTICLE

## Teratoma pathology and genomics in anti-NMDA receptor encephalitis

Yoonhyuk Jang<sup>1,\*</sup>, Kwanghoon Lee<sup>2,\*</sup>, Cheol Lee<sup>2,\*</sup>, Kon Chu<sup>1</sup> , Sang Kun Lee<sup>1</sup> ,  
Jae-Kyung Won<sup>2</sup> & Soon-Tae Lee<sup>1</sup> <sup>1</sup>Department of Neurology, Seoul National University Hospital, Seoul National University College of Medicine, Seoul, South Korea<sup>2</sup>Department of Pathology, Seoul National University Hospital, Seoul National University College of Medicine, Seoul, South Korea

## Correspondence

Soon-Tae Lee, Department of Neurology,  
Seoul National University Hospital, Seoul  
National University College of Medicine, 101  
Daehak-ro, Jongno-gu, Seoul 03080, South  
Korea. Tel: +82-2-2072-4757; E-mail:[staelee@snu.ac.kr](mailto:staelee@snu.ac.kr)

and

Jae-Kyung Won, Department of Pathology,  
Seoul National University Hospital, Seoul  
National University College of Medicine, 101  
Daehak-ro, Jongno-gu, Seoul 03080, South  
Korea. Tel: +82-2-2072-4895; E-mail:[jkwon@snuh.org](mailto:jkwon@snuh.org)

## Funding Information

This work was supported by a National  
Research Foundation of Korea (NRF) grant  
funded by the Ministry of Science and ICT  
(2022R1A2B5B01001331) and a grant of the  
Korea Health Technology R&D Project  
through the Korea Health Industry  
Development Institute (KHIDI) funded by the  
Ministry of Health & Welfare (RS-2023-  
00266044), Republic of Korea. Y.J. and S-T.L.  
were supported by Lee Sueng Moon  
Research Fund of Seoul National University  
Hospital (3020170130).Received: 16 September 2023; Revised: 31  
October 2023; Accepted: 3 November 2023*Annals of Clinical and Translational  
Neurology* 2024; 11(1): 225–234

doi: 10.1002/acn3.51948

\*These authors contributed equally to this  
study as co-first authors.

## Introduction

Anti-N-methyl-D-aspartic acid receptor encephalitis  
(NMDAR) is the most common and severe type of

## Abstract

**Introduction:** Ovarian teratoma is a common occurrence in patients with anti-NMDA receptor encephalitis (NMDAR), and its removal is crucial for a favorable prognosis. However, the initial pathogenesis of autoimmunity in the encephalitic teratoma remains unclear. In this study, we aimed to investigate the genomic landscape and microscopic findings by comparing NMDAR-associated teratomas and non-encephalitic control teratomas. **Materials and Methods:** A prospective consecutive cohort of 84 patients with NMDAR was recruited from January 2014 to April 2020, and among them, patients who received teratoma removal surgery at Seoul National University Hospital were enrolled. We conducted a comparison of whole-exome sequencing data and pathologic findings between NMDAR-associated teratomas and control teratomas. **Results:** We found 18 NMDAR-associated teratomas from 15 patients and compared them with 17 non-encephalitic control teratomas. Interestingly, the genomic analysis revealed no significant differences in mutations between encephalitic and non-encephalitic teratomas. Pathologic analysis showed no discrepancies in terms of the presence of neuronal tissue and lymphocytic infiltration between the encephalitic teratomas ( $n = 14$ ) and non-encephalitic teratomas ( $n = 18$ ). However, rituximab-naïve encephalitic teratomas exhibited a higher frequency of germinal center formation compared to non-encephalitic teratomas (80% vs. 16.7%,  $P = 0.017$ ). Additionally, rituximab-treated encephalitic teratomas demonstrated a reduced number of CD20<sup>+</sup> cells and germinal centers in comparison to rituximab-naïve encephalitic teratomas ( $P = 0.048$  and 0.023, respectively). **Discussion:** These results suggest that the initiation of immunopathogenesis in NMDAR-associated teratoma is not primarily attributed to intrinsic tumor mutations, but rather to immune factors present in the encephalitic patient group, ultimately leading to germinal center formation within the teratoma.

autoimmune encephalitis, caused by autoantibodies  
against the NR1 subunit of NMDAR on the neuronal cell  
surface.<sup>1</sup> Ovarian teratoma is found in approximately  
40% of patients,<sup>2</sup> in which the teratoma has NR1

expression and a germinal center leading to B-cell activation and antibody production.<sup>3,4</sup> Accordingly, rapid removal of the ovarian teratoma, in addition to early adjuvant immunotherapy, is essential for patients' recovery.<sup>2,5,6</sup> However, in the majority of NMDARe patients without teratoma, other than the fact that B cells in cervical lymph nodes are NR1-reactive in some patients,<sup>3</sup> the immunogenic cause is largely unknown.

In order to understand the immune recognition of NR1 in the NMDARe, it is crucial to analyze where the driver of autoimmunity comes from, and why immune recognition of teratoma or encephalitis-induced antigens occurs only in a small portion of the patients. While ovarian teratoma has been spotlighted as the key to the pathogenesis, mature cystic teratoma is not uncommon in young adults, accounting for 20% of all ovarian tumors,<sup>7,8</sup> and is generally asymptomatic in terms of paraneoplastic syndrome. Attempts have been made to evaluate the pathological differences of ovarian teratoma in NMDARe compared to control teratoma,<sup>9,10</sup> and ovarian teratoma is a nest where NMDAR-autoantibody-producing B cells form germinal centers.<sup>3,4</sup> Nevertheless, why immune cells recognize the NR1-autoantigen has not been clearly elucidated, which is the key to explaining NMDARe patients in the selected teratoma population, and may explain about the non-teratoma population.

Therefore, this study aimed to analyze the genomic landscape between NMDARe-associated teratomas and non-encephalitic teratomas. In the event of a difference in genomic mutations, the pathogenesis of NMDARe can be explicated. Conversely, the absence of such genomic mutations would suggest that the difference in the expression of the tumor-specific antigen is not the cause of the autoimmunity, but rather the differential recognition of the tumor by immune factors might be responsible.

## Methods

### Patient enrollment, antibody determination, and teratoma selection

A prospective consecutive cohort of 84 patients with NMDARe was recruited from January 2014 to April 2020, and among them, patients who received teratoma removal surgery with informed consent at Seoul National University Hospital were selected (Figure S1). We identified the presence of anti-NMDAR antibodies in the serum and cerebrospinal fluid of patients using immunohistochemistry staining of rat brain sections and a cell-based immunocytochemistry assay kit (Euroimmune Ag, Germany), as described in our previous studies.<sup>11,12</sup> In the same period, 508 non-encephalitic control patients who had

surgery due to ovarian teratoma were reviewed and 1:2 age-matched with the chosen patients with NMDARe. Through the medical and pathology review, control patients who had available teratoma tissue were finally analyzed. Then, we also analyzed available peripheral blood mononuclear cells from the selected encephalitis group. This study was approved by the Seoul National University Hospital Institutional Review Board and written informed consent was obtained from all patients and/or legal guardians.

### Clinical assessment

The clinical information about NMDARe patients was evaluated with the duration from the disease onset to immunotherapy, from the onset to tumor removal, and outcome assessment with the following scales: Clinical Assessment Scale for autoimmune Encephalitis (CASE),<sup>13</sup> modified Rankin Scale (mRS), and NMDARe One-year functional Status (NEOS).<sup>14</sup>

### Sample preparation and data generation

We selected tissue slices that have neuroglial components and germinal centers, and the entire tissue piece was submitted for analysis. DNA was extracted from formalin-fixed paraffin-embedded ovarian teratoma using Maxwell<sup>®</sup> FFPE Plus DNA Kit (Promega, AS1720), while peripheral blood DNA was extracted using ReliaPrep<sup>™</sup> gDNA Tissue Miniprep System (A2051). To generate standard exome capture libraries, we used the Agilent SureSelectXT Low Input Target Enrichment protocol for Illumina paired end sequencing library with 1 µg of input gDNA. For exome capture, 250 ng of DNA library was mixed with hybridization buffers, blocking mixes, RNase block, and 5 µL of SureSelect all exon capture library, according to the standard Agilent SureSelect Target Enrichment protocol. The quality control criteria included a minimum of 0.500 µg of sample DNA with a DIN of 7, and a library DNA concentration of 10 nmol/L. The sequencing was performed with a depth of 100× (Tables S1 and S2). The base calling files, which are expressed in binary, were converted to FASTQ using the Illumina package bcl2fastq v2.20.0.

### Whole-exome sequencing data analysis

The sequencing quality was checked using FastQC, followed by mapping of paired end sequences to the human reference genome hg19 using the "Burrows-Wheeler Alignment" tool. Duplicate reads were removed, and base quality scores were recalibrated using the Genome

Analysis Toolkit (GATK, <http://www.broadinstitute.org/gatk>). Variants were then called and filtered using GATK, with annotations performed using SnpEff and filtering applied using dbSNP and SNPs from the 1000 genome project, as well as other databases including ClinVar. CNV analysis was carried out using CNVkit. To filter variants, we employed multiple criteria. First, variants with a mapping quality score below 60 were excluded. Additionally, variants classified as “synonymous\_variant” and non-exonic variants, such as “intron\_variant” and “intergenic\_region,” were removed from consideration. We also selected variants with an allele frequency <1% in the 1000 Genomes database. For CLINVAR\_CLNSIG criteria, we only selected variants classified as “Pathogenic,” “Likely\_Pathogenic,” or “Uncertain\_significance.” All candidates were manually reviewed using the Integrative Genomics Viewer. For somatic mutations, we utilized the “Haplotype Caller” for variant calling. To distinguish somatic mutations from germline ones, we also analyzed the mutations on matched blood DNA samples from the encephalitis group. Mutational signature analysis was conducted using the web tool MUTALISK (<http://mutalisk.org/>).<sup>15</sup> Clinical information and mutations were summarized using Oncoprint data, which were generated using the R package “ComplexHeatmap” (version 2.7.6.1002).<sup>16</sup>

## Pathology analysis

Representative blocks were selected through the review of all hematoxylin and eosin slides. All immunohistochemistry staining was performed on 4  $\mu$ m sections of representative blocks using a Benchmark XT stainer (Ventana/Roche Tissue Diagnostics, Indianapolis, IN, USA) according to the manufacturers' guidelines. Primary antibodies were antigial fibrillary acidic protein (GFAP) (M0761, DAKO, 1:200), anti-CD45 (LCA) (M0701, DAKO, 1:600), anti-CD3 (790-4341, VENTANA, RTU), anti-CD20 (M0755, DAKO, 1:500), anti-CD4 (790-4423, VENTANA, RTU), anti-CD8 (790-4460, VENTANA, RTU), anti-Bcl6 (Bcl-6-564, Novocastra, 1:80), anti-CD10 (PA0270, Novocastra, RTU), anti-CD21 (NCL-L-CD21-2G9, Novocastra, 1:50), anti-FOXP3 (ab20034, Abcam, 1:200), and anti-NR1 (ab193310, Abcam, 1:200).

The germinal center formation was determined by integrating findings of CD20 as a B-cell marker, Bcl6 and CD10 as germinal center markers, and CD21 as a follicular dendritic cell marker. The ratio of GFAP-positive area, CD45-positive immune cell count, NR1, CD3, CD20, CD4, and CD8-positive cell numbers and each ratio were analyzed through digital scanning using Aperio GT450 slide scanner (Leica Biosystems, Buffalo Grove, IL, USA) and measurement using QuPath software (QuPath version 0.3.2).

## Statistical analysis

Data are presented as the mean  $\pm$  SD (range), median (IQR), or number (%). Statistical analyses were conducted using R software v.4.3.0 (2023; R team, Vienna, Austria). Significance was defined as a  $P < 0.05$ . Intergroup comparisons for continuous variables were performed using  $t$  tests or Mann–Whitney  $U$ -tests, while Fisher's exact test was used for categorical variables.

## Results

### Clinical characteristics of patients

Out of 84 patients with NMDARe, 31 patients underwent teratoma removal surgery, and among them, teratoma tissue was available from 15 patients who provided informed consent. All teratoma were mature teratomas. Of 508 non-encephalitic control patients with ovarian teratoma, we selected 18 patients who were matched for age (Table 1, Table S3–S5, Figure S1). The mean age of the patients with NMDARe and the controls was  $23.9 \pm 6.4$  (range: 17–37) and  $24.4 \pm 6.2$  (16–38), respectively. The patients with NMDARe had a poor initial clinical profile showing a median NEOS score of 3 (interquartile range: 2–4), a median CASE score of 22 (19–23), and a median mRS score of 5 [5]. The mean duration from symptom onset to teratoma removal was  $60.6 \pm 83.0$  days (ranged from 10 to 300). Before the tumor removal, all the patients received first-line immunotherapy (corticosteroid or intravenous immunoglobulin), while 53.3% (8 out of 15) of the patients received rituximab as a second-line treatment. After treatment, the patients with NMDARe had favorable final outcomes at their last follow-up, with a median CASE score of 1 (0–2) and a median mRS score of 1 (0–1).

### Mutation signatures of NMDARe-associated teratoma

The whole-exome sequencing (WES) analysis in 18 encephalitic and 17 non-encephalitic teratomas showed no significant differences in the canonical mutation analysis between the two groups (Fig. 1, Tables S3 and S6), suggesting that the two types of tumors are genetically not different. Sporadic mutations were observed in both groups, with the most common finding being a missense mutation in CD36. However, there was no significant difference in the frequency of this mutation between the groups (3 out of 18 [16.7%] for NMDARe teratomas vs. 5 out of 17 [29.4%] for control teratomas,  $P = 0.443$ ). In NMDARe teratomas, the mean variant allele frequency of

**Table 1.** Demographics and characteristics of patients with anti-NMDAR encephalitis and ovarian teratoma.

Clinical profiles	Anti-NMDAR encephalitis ( <i>n</i> = 15)	2-year outcome (mRS > 2)		<i>P</i> -value (good vs. poor)
		Good ( <i>n</i> = 8)	Poor ( <i>n</i> = 7)	
Age (years)	23.9 ± 6.4 [17–37]	25.8 ± 7.5 [17–37]	21.9 ± 4.6 [17–28]	0.244
Initial clinical profiles				
NEOS scores	3 [2–4]	2 [1–2]	4 [3–4]	0.023*
CASE scores	22 [19–23]	20 [19–22]	22 [22]	0.307
mRS scores	5 [5]	5 [5]	5 [5]	N/A
CSF profiles at worst				
Leukocyte level (cells/μL)	52.9 ± 51.7	46.5 ± 52.0	60.1 ± 54.4	0.630
Protein level (mg/dL) ( <i>n</i> = 14)	40.1 ± 15.4	45.6 ± 13.7	35.5 ± 16.2	0.230
Brain MRI abnormality (%)	7 (46.7)	2 (25)	4 (57.1)	0.315
Treatment profiles				
Onset to immunotherapy (days)	12.3 ± 6.6	14.0 ± 8.3	10.3 ± 3.2	0.273
Steroid (%)	11 (73.3)	6 (75)	5 (71.4)	0.843
IVIg (%)	14 (93.3)	7 (87.5)	7 (100)	1
Rituximab (%)	8 (53.3)	3 (37.5)	5 (71.4)	0.315
Tocilizumab (%)	4 (26.7)	1 (12.5)	3 (42.9)	0.282
Others (cytoxan, azathioprine) (%)	2 (13.3)	0	2 (28.6)	0.200
Delayed teratoma removal (%)	6 (40)	3 (37.5)	3 (42.9)	
Duration from diagnosis to removal (days)	60.6 ± 83.0	34.3 ± 32.4	90.7 ± 113.5	0.245
Rituximab before teratoma removal (%)	8 (53.3)	3 (37.5)	5 (71.4)	0.315
Outcomes profiles				
2-year CASE scores	4 [1–11]	1 [1]	11 [8–14]	
2-year mRS scores	2 [1–4]	1 [1]	4 [4]	
Final CASE scores	1 [0–2]	0 [0–1]	1 [0–3]	0.322
Final mRS scores	1 [0–1]	0 [0–1]	1 [0–2]	0.272
Genetic profiles <sup>a</sup>				
Sequenced teratoma sample ( <i>n</i> )	18	9	9	
CD36 (%)	3 (16.7)	2 (22.2)	1 (11.1)	1
PADI3 (%)	2 (11.1)	2 (22.2)	0	0.471
TEX11 (%)	2 (11.1)	2 (22.2)	0	0.471
Pathology profiles				
Analyzed pathology sample ( <i>n</i> )	14	7	7	
Rituximab-naïve teratoma ( <i>n</i> )	5	4	1	
Tumor size (mm)	30.7 ± 23.2	29.3 ± 15.5	32.1 ± 30.3	0.829
GFAP+ area (%)	5.30 ± 6.22	7.96 ± 7.67	2.64 ± 2.87	0.126
NR1+ cells/HPF	23.9 ± 60.9	11.8 ± 16.3	36.0 ± 86.2	0.491
GC formation (%)	5 (35.8)	4 (57.1)	1 (14.2)	0.266
GC formation in rituximab-naïve teratoma (%)	4 (80)	3 (75)	1 (100)	1
CD45 <sup>+</sup> cells/HPF	231.6 ± 247.7	338.0 ± 274.3	125.2 ± 176.6	0.113
CD20 <sup>+</sup> cells/HPF	161.3 ± 276.7	214.1 ± 288.2	108.6 ± 276.3	0.498
CD3 <sup>+</sup> cells/HPF	198.2 ± 246.2	224.6 ± 286.7	171.7 ± 218.0	0.705
CD4 <sup>+</sup> cells/HPF	243.4 ± 261.6	255.4 ± 281.3	231.5 ± 262.2	0.872
CD8 <sup>+</sup> cells/HPF	181.5 ± 228.2	262.7 ± 299.4	100.3 ± 88.0	0.211
CD4 <sup>+</sup> cells/CD3 <sup>+</sup> cells ratio	4.21 ± 10.20	1.69 ± 1.14	6.77 ± 14.5	0.385
CD8 <sup>+</sup> cells/CD3 <sup>+</sup> cells ratio	3.18 ± 5.64	2.42 ± 3.52	3.95 ± 7.43	0.636
CD3 <sup>+</sup> cells/CD20 <sup>+</sup> cells ratio	59.14 ± 126.21	80.4 ± 173.4	34.3 ± 27.8	0.513
CD4 <sup>+</sup> cells/CD8 <sup>+</sup> cells ratio	2.02 ± 2.98	1.39 ± 1.05	2.65 ± 4.15	0.463

Data are presented as mean ± SD (range) or as median (IQR). CASE, clinical assessment scale for autoimmune encephalitis; CSF, cerebrospinal fluid; IVIg, intravenous immunoglobulin; mRS, modified Rankin Scale; MRI, magnetic resonance imaging; NEOS, the NMDAR One-Year Functional Status; NMDAR, N-methyl-D-aspartic acid receptor; SD, standard deviation.

<sup>a</sup>Genetic mutations observed in two or more teratomas were selected.

\**P* < 0.05.

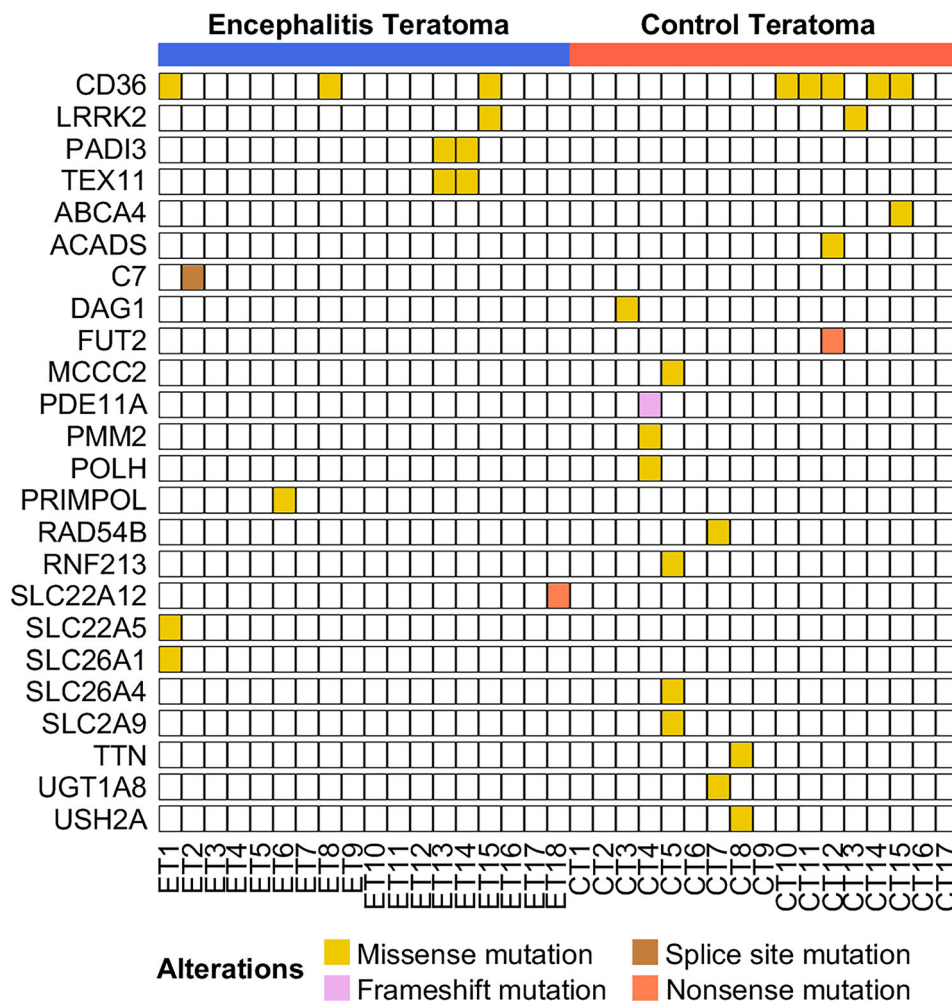


**Figure 1.** The oncoplot comparing NMDAR teratoma and control teratoma using tumor-only data. There was no difference in the mutation profiles between the two groups ( $n = 18$  for the encephalitis group and  $n = 17$  for the control group). Sporadic mutations were observed in specific genes, including CD36, LRRK2, PADI3, and TEX11, with missense mutations being the most common type of alteration. The most frequently occurring mutation in both groups was a missense mutation in CD36. However, there was no significant difference in mutation frequency between the NMDAR teratoma group (3 out of 18, 16.7%) and the control teratoma group (5 out of 18, 29.4%) ( $P = 0.443$ ). All gene variants were selected based on the population allele frequency  $<0.01$  (1%) and other criteria (see “Method”). NMDAR, N-methyl-D-aspartic acid receptor; anti-NMDAR encephalitis, NMDAR.

single-nucleotide variations and insertion–deletion mutations was higher compared to their matched peripheral blood, which might be associated with tumorigenesis (Figure S2). However, in comparison between the encephalitic teratoma and the control teratoma, there was no difference in the mean variant allele frequency of single-nucleotide variations and insertion–deletion mutations, indicating that the two types of teratoma had no difference in the amount of mutation burden.

We further analyzed WES by comparing encephalitic teratomas with their available blood samples ( $n = 11$ , Table S3, Figure S3). Although some variants in tumor met the statistical threshold, they were not clinically significant, as no matches were found in the comparison

between the encephalitic and control teratomas. We also performed mutational signature analysis to detect any underlying mutational processes that may have shaped a particular set of genomic alterations in encephalitic teratomas,<sup>15</sup> but did not find any significant single-base substitution patterns in the genomic mutation landscape (Figures S4 and S5).

### Pathologic differences between encephalitic and non-encephalitic teratomas.

For the next step, we investigated the pathology of 14 encephalitic and 18 non-encephalitic teratomas (Table 2, Fig. 2, Table S3). Teratomas in the control group were



**Table 2.** Pathology analysis of patients with ovarian teratoma.

Pathology profiles	Total anti-NMDAR encephalitis teratoma	Rituximab-naïve encephalitic teratoma	Rituximab-treated encephalitic teratoma	Control	<i>P</i> -value (total vs. control)	<i>P</i> -value (rituximab-naïve vs. control)	<i>P</i> -value (rituximab-naïve vs. Rituximab-treated)
Analyzed pathology sample ( <i>n</i> )	14	5	9	18			
Tumor size (mm)	30.7 ± 23.2	32.2 ± 17.4	29.9 ± 26.9	99.8 ± 76.2	0.003**	0.003**	0.849
GFAP+ area (%)	5.30 ± 6.22	7.12 ± 8.48	4.29 ± 4.86	25.02 ± 25.67	0.009**	0.021*	0.521
NR1+ cells/HPF	23.9 ± 60.9	61.5 ± 96.2	2.97 ± 5.68	13.9 ± 39.7	0.580	0.335	0.245
GC formation (%)	5 (35.8)	4 (80)	1 (11.1)	3 (16.7)	0.230	0.017*	0.023*
CD45 <sup>+</sup> cells/HPF	231.6 ± 247.7	433.1 ± 270.8	119.6 ± 153.3	297.7 ± 506.9	0.658	0.441	0.058
CD20 <sup>+</sup> cells/HPF	161.3 ± 276.7	427.6 ± 330.2	13.4 ± 30.7	294.2 ± 613.2	0.458	0.530	0.048*
CD3 <sup>+</sup> cells/HPF	198.2 ± 246.2	161.5 ± 185.9	218.5 ± 282.7	182.3 ± 253.0	0.860	0.843	0.658
CD4 <sup>+</sup> cells/HPF	243.4 ± 261.6	224.9 ± 225.0	253.7 ± 292.4	225.4 ± 289.4	0.857	0.996	0.841
CD8 <sup>+</sup> cells/HPF	181.5 ± 228.2	307.7 ± 347.4	111.4 ± 93.5	144.7 ± 113.9	0.555	0.356	0.278
CD4 <sup>+</sup> cells/CD3 <sup>+</sup> cells ratio	4.21 ± 10.20	1.84 ± 1.33	5.52 ± 12.7	1.42 ± 1.33	0.258	0.551	0.416
CD8 <sup>+</sup> cells/CD3 <sup>+</sup> cells ratio	3.18 ± 5.64	3.00 ± 4.11	3.29 ± 6.58	1.53 ± 1.32	0.236	0.472	0.921
CD3 <sup>+</sup> cells/CD20 <sup>+</sup> cells ratio	59.14 ± 126.21	1.37 ± 1.68	95.2 ± 153.1	3.03 ± 3.13	0.076	0.146	0.126
CD4 <sup>+</sup> cells/CD8 <sup>+</sup> cells ratio	2.02 ± 2.98	1.10 ± 0.75	2.53 ± 3.65	1.60 ± 1.62	0.609	0.345	0.285

Data are presented as mean ± SD.

Abbreviations: GC, germinal center; GFAP, glial fibrillary acidic protein; HPF, high-power field; NMDAR, N-methyl-D-aspartic acid receptor.

\**P* < 0.05.

\*\**P* < 0.01.

significantly larger and had a greater area of GFAP-positive cells. However, when we analyzed the NR1 expression in all type cells, there were no significant differences in the distribution of NR1-positive cells or immune cells between the two groups. The number of NR1-positive cells per high-power field (HPF) was comparable between the encephalitis and control groups (*P* = 0.580). When we compared the two teratoma groups regardless of background immunologic treatments, the frequency of germinal center formation was also similar in both groups, with five samples (5 out of 14, 35.8%) in the encephalitis group and three samples (3 out of 18, 16.7%) in the control group (*P* = 0.230). Additionally, the extent and subtypes of leukocyte infiltration into the teratoma tissue were not different between the encephalitis and control teratomas.

As rituximab treatment could influence the frequency of germinal center detection and CD20<sup>+</sup> cell counts, we then analyzed the NMDAR<sup>e</sup> teratomas separating rituximab-treated encephalitic teratomas from rituximab-naïve encephalitic teratomas (*n* = 9 and *n* = 5, respectively, Table 2). The rituximab-treated encephalitic teratomas exhibited lower CD20<sup>+</sup> cell counts compared to the rituximab-naïve encephalitic teratomas (*P* = 0.048). Furthermore, a lower incidence of germinal center formation was observed in the rituximab-treated encephalitic teratomas compared to the rituximab-naïve encephalitic teratomas (*P* = 0.023). Notably, the rituximab-naïve encephalitic teratomas displayed a higher occurrence of

germinal center formation compared to the non-encephalitic control teratomas (*P* = 0.017). This result is consistent with the previous study,<sup>3</sup> indicating that germinal center formation represents the primary pathologic distinction between NMDAR<sup>e</sup> teratomas and control teratomas, reflecting the generation of antibodies within the tumor.

### Association with prognosis of patients with NMDAR<sup>e</sup>

To investigate the potential association of genetic mutations or pathological characteristics with the prognosis of patients with NMDAR<sup>e</sup>, we classified the patients based on their mRS scores at the 2-year follow-up (Table 1). The group with a poor outcome (mRS > 2 at 2-year follow-up, *n* = 7) did not show any significant differences in clinical profiles compared to the group with a good outcome (mRS ≤ 2 at 2-year follow-up, *n* = 8), except for the NEOS score (*P* = 0.023). Moreover, there were no significant differences observed in the analysis of genetic mutations or the examination of pathological features between the two groups.

### Discussion

Here, we analyzed whole-exome sequencing and pathology in 18 teratomas from NMDAR<sup>e</sup> and 17 teratomas from control, and found that the NMDAR<sup>e</sup>-associated

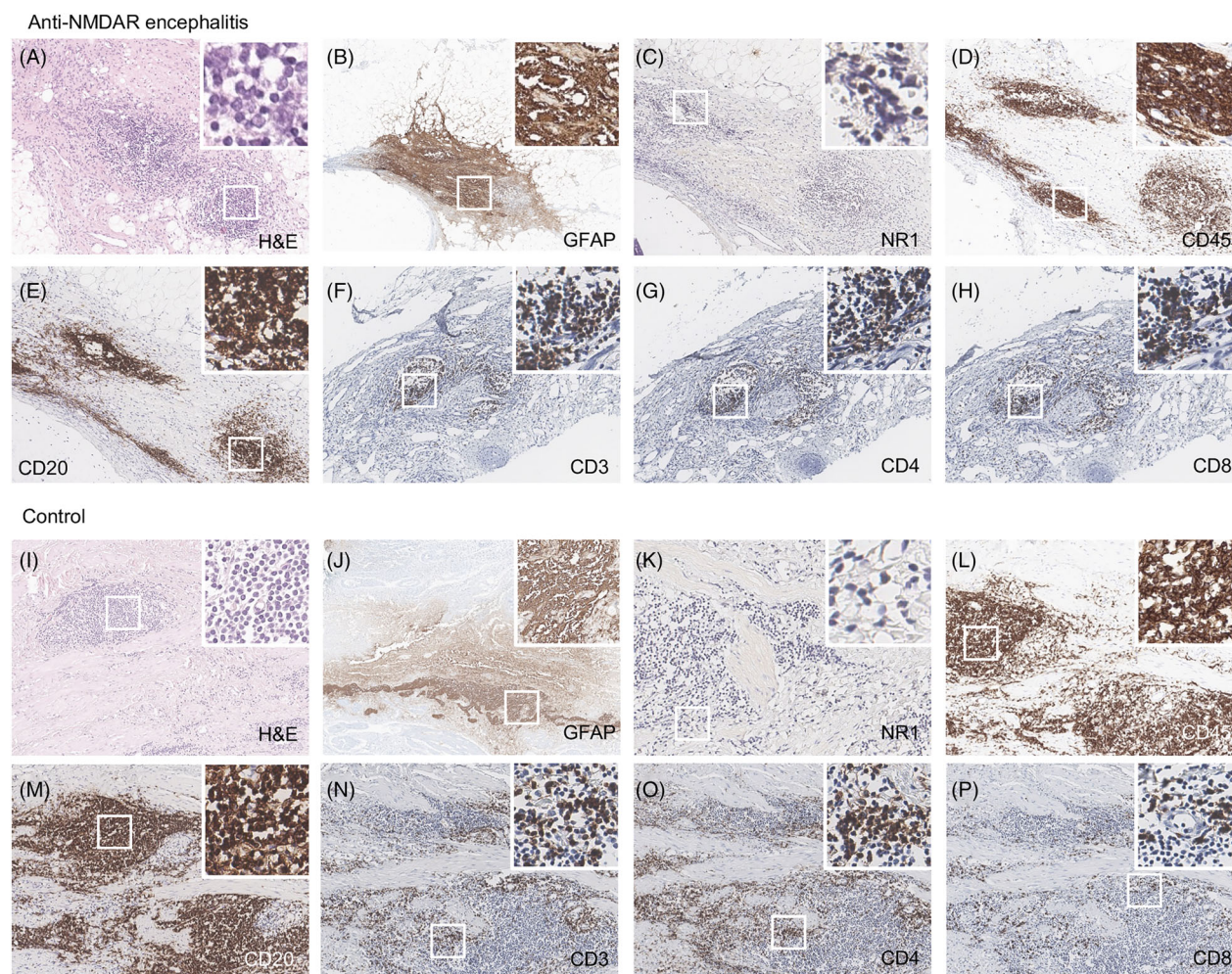


**Figure 2.** Pathology finding of ovarian teratomas from NMDAR and controls. (A–H) Teratomas from patients with NMDAR. (A) H&E staining shows lymphocyte infiltration ( $\times 200$ ). (B) Abundant neuroglia positivity in GFAP staining ( $\times 100$ ). (C) NR1 positivity was shown ( $\times 400$ ). (D–H) Immune cells were diffusely infiltrated. (D) CD45 ( $\times 200$ ). (E) CD20 ( $\times 200$ ). (F) CD3 ( $\times 200$ ). (G) CD4 ( $\times 200$ ). (H) CD8 ( $\times 200$ ). (I–P) Teratomas from controls. NR1-positive cells and immune cell infiltration were similarly observed compared to NMDAR-associated teratomas. (I) H&E staining ( $\times 200$ ). (J) GFAP staining ( $\times 100$ ). (K) NR1 staining ( $\times 400$ ). (L) CD45 ( $\times 200$ ). (M) CD20 ( $\times 200$ ). (N) CD3 ( $\times 200$ ). (O) CD4 ( $\times 200$ ). (P) CD8 ( $\times 200$ ). GFAP, glial fibrillary acidic protein; H&E, hematoxylin and eosin.

teratomas showed no significant genetic differences compared to the control teratomas. The NMDAR-associated teratomas appear not to have any inborn canonical mutations compared to the control teratomas. These data suggest that the ignition of immunopathogenesis to teratoma may not be due to intrinsic tumor mutations, but rather to immune factors. In pathologic analysis, the rituximab-naïve NMDAR teratomas had a higher frequency of germinal center formations compared to the control teratomas. Given that NR1 expression and lymphocytic infiltration did not show any differences between the encephalitic and non-encephalitic teratomas, the pathogenic steps occurring between lymphocytic infiltration and germinal center formation may play a critical role in

the induction of encephalitis by teratomas, which remains to be elucidated.

So far, how NR1 antigen is initially recognized to produce anti-NR1 antibody in NMDAR has not been clearly identified yet. Several attempts have been made to elucidate the very initial pathogenesis of autoimmunity, but have not been successful. Our study demonstrates that the serial pathologic process, including mutations, NR1 expression, and lymphocytic infiltration, does not differ between control teratomas and NMDAR-associated teratomas. However, the two types of tumors diverge at the stage of germinal center formation. Furthermore, the observed lymphocytic infiltration and gene mutations in encephalitic teratomas did not show a significant



association with patients' prognosis, suggesting that the genetic and pathologic features of teratomas do not exert a substantial influence on the immune response triggering encephalitis. Instead, these findings support that the pathogenic steps beyond NR1-specific germinal center formation within the teratoma play a crucial role in shaping the characteristics of autoimmunity.

Meanwhile, the teratomas in the NMDARe group were significantly smaller in size compared to those in the control group. In the control group, teratomas were typically removed when they reached a specific size or when they caused symptoms due to mass effect. In contrast, the NMDARe teratomas were detected early by their immunogenicity, even in their very early stages, and were removed without the presence of mass effects. This difference in detection and management approaches is likely the key factor contributing to the observed differences in teratoma sizes between the control and NMDARe groups. In addition, although all NMDARe teratoma were mature teratoma in this study, immature teratomas can also drive the encephalitis.<sup>17</sup>

Previous studies have shown the existence of NR1-specific immunoglobulin G (IgG) in the germinal center of ovarian teratoma in patients with NMDARe.<sup>3,4</sup> Moreover, NR1-specific B cells and IgG were identified in the cervical lymph nodes of the patients, providing evidence that ovarian teratoma-driven inflammation could cause central nervous system autoimmunity via this route.<sup>3</sup> However, contrary to previous autopsy cases,<sup>18</sup> our study revealed that the infiltration of immune cells, including CD20<sup>+</sup> B lymphocytes, into teratoma tissue is similar in both the encephalitis and control groups. Because NR1-specific autoantibodies have never been found in ovarian teratoma patients without encephalitis symptoms,<sup>19</sup> the germinal centers discovered in non-encephalitic teratoma might not be related to NR1-antibody.

Hence, it is plausible to suggest that certain susceptible individuals may harbor systemic or immune-intrinsic factors that facilitate immune recognition of teratomas, thus leading to autoimmunity and germinal center formation. This could potentially explain why only a minority of patients with herpes encephalitis (18%) go on to develop NMDARe, despite the hippocampal NR1 antigen being capable of draining to deep cervical lymph nodes theoretically in all herpes encephalitis.<sup>20</sup> Similarly, among 93 individuals who had post-herpes simplex virus encephalitis, 39 patients (42%) were found to have neuronal antibodies, including anti-NR1 antibodies, and 21 of them (22.6%) developed autoimmune encephalitis. Notably, some of these patients exhibited specific host factors, such as particular HLA alleles and mutations in Type I interferon-related genes.<sup>21</sup> In addition, some of these vulnerable patients may experience germinal center reactions

in systemic sites such as cervical lymph nodes, even in the absence of a teratoma. This hypothesis provides a plausible explanation for the development of NMDARe in non-teratoma patients.

Further research is required to evaluate posttranscriptional modification in generating NR1 neoantigens within NMDARe-associated teratoma. Moreover, to further validate our study, whole-genome sequencing would be an additional tool to investigate intronic variations near splicing sites, patterns similar to those observed in tumors associated with anti-Yo antibodies.<sup>22</sup> Considering that a genome-wide study suggested candidate peripheral blood genes associated with B cell development,<sup>23</sup> it is also important to identify other immune cell-intrinsic etiologies from peripheral blood. In contrast to leucine-rich glioma inactivated1-antibody encephalitis,<sup>24,25</sup> NMDARe has no specific human leukocyte antigen (HLA) subtypes.<sup>26</sup> Single-cell transcriptomics may offer valuable insights by allowing the assessment of transcription levels in individual immune cells responsive to teratomas. Further elucidating the pathogenesis of autoimmunity in non-teratoma NMDARe patients can enhance our understanding of the pathogenesis and refractoriness of NMDARe.

## Author Contributions

Y.J. and S-T.L. drafted the manuscript. C.L. and J-K.W. revised the manuscript. Y.J. and C.L. prepared tables. Y.J. and G.L. prepared figures. Y.J. and S-T.L. reviewed patients medical records. G.L. and J-K.W. analyzed the sequencing data. C.L. and J-K.W. analyzed the pathology. S-T.L. analyzed the autoantibody tests. S-T.L., K.C., and S.K.L. collected clinical data. S-T.L. provided study concepts. S-T.L. and J-K.W. supervised the study. All authors reviewed the manuscript.

## Conflicts of interest

The authors declare that they have no competing interests.

## Disclosures

S-T. L. receives research grants from GC pharma and autoimmune encephalitis alliance to Seoul National University Hospital. S-T. L. receives consulting fees from Advanced Neural Technologies.

## Data availability statement

Anonymized data that support the findings of this study are available from the corresponding author upon



reasonable request of any qualified investigator for purposes of replicating procedures and results. If such data are used for a publication, its methods should be communicated, and internationally recognized authorship rules should be applied.

## Ethics approval and consent to participate

This study was approved by the Seoul National University Hospital Institutional Review Board (IRB no. 1705-130-856) and written informed consent was obtained from all patients and/or legal guardians. All co-authors have reviewed and approved the contents of the manuscript, and the *Annals of Clinical and Translational Neurology* requirements for authorship have been met. We confirm that we have read the journal's position on issues related to ethical publication and affirm that this report is consistent with those guidelines. We certify that the submission (aside from an abstract) is not under review by any other publication. No previous report overlaps with the current work. We have no conflicts of interest to declare.

## References

- Dalmau J, Graus F. Antibody-mediated encephalitis. *N Engl J Med*. 2018;378(9):840-851.
- Titulaer MJ, McCracken L, Gabilondo I, et al. Treatment and prognostic factors for long-term outcome in patients with anti-NMDA receptor encephalitis: an observational cohort study. *Lancet Neurol*. 2013;12(2):157-165.
- Al-Diwani A, Theorell J, Damato V, et al. Cervical lymph nodes and ovarian teratomas as germinal centres in NMDA receptor-antibody encephalitis. *Brain*. 2022;145(8):2742-2754.
- Makuch M, Wilson R, Al-Diwani A, et al. N-methyl-D-aspartate receptor antibody production from germinal center reactions: therapeutic implications. *Ann Neurol*. 2018;83(3):553-561.
- Lee W-J, Lee S-T, Shin Y-W, et al. Teratoma removal, steroid, IVIG, rituximab and tocilizumab (T-SIRT) in anti-NMDAR encephalitis. *Neurotherapeutics*. 2021;18:474-487.
- Lee S-T. Symptomatic treatments of N-methyl-D-aspartate receptor encephalitis. *Encephalitis*. 2021;1(1):4-6.
- Westhoff C, Pike M, Vessey M. Benign ovarian teratomas: a population-based case-control study. *Br J Cancer*. 1988;58(1):93-98.
- Berek JS, Hacker NF, Hengst TC. Practical gynecologic oncology. Lippincott Williams & Wilkins; 2005.
- Day GS, Laiq S, Tang-Wai DF, Munoz DG. Abnormal neurons in teratomas in NMDAR encephalitis. *JAMA Neurol*. 2014;71(6):717-724.
- Nolan A, Buza N, Margeta M, Rabban JT. Ovarian teratomas in women with anti-N-methyl-D-aspartate receptor encephalitis: topography and composition of immune cell and neuroglial populations is compatible with an autoimmune mechanism of disease. *Am J Surg Pathol*. 2019;43(7):949-964.
- Lee W-J, Lee S-T, Byun J-I, et al. Rituximab treatment for autoimmune limbic encephalitis in an institutional cohort. *Neurology*. 2016;86(18):1683-1691.
- Lee WJ, Lee HS, Kim DY, et al. Seronegative autoimmune encephalitis: clinical characteristics and factors associated with outcomes. *Brain*. 2022;145(10):3509-3521.
- Lim JA, Lee ST, Moon J, et al. Development of the clinical assessment scale in autoimmune encephalitis. *Ann Neurol*. 2019;85(3):352-358.
- Balu R, McCracken L, Lancaster E, Graus F, Dalmau J, Titulaer MJ. A score that predicts 1-year functional status in patients with anti-NMDA receptor encephalitis. *Neurology*. 2019;92(3):e244-e252.
- Lee J, Lee Andy J, Lee J-K, et al. Mutalisk: a web-based somatic MUTation AnaLyIS toolKit for genomic, transcriptional and epigenomic signatures. *Nucleic Acids Res*. 2018;46(W1):W102-W108.
- Gu Z, Eils R, Schlesner M. Complex heatmaps reveal patterns and correlations in multidimensional genomic data. *Bioinformatics*. 2016;32(18):2847-2849.
- Ación P, Ación M, Ruiz-Maciá E, Martín-Estefanía C. Ovarian teratoma-associated anti-NMDAR encephalitis: a systematic review of reported cases. *Orphanet J Rare Dis*. 2014;9(1):157.
- Tüzün E, Zhou L, Baehring JM, Bannykh S, Rosenfeld MR, Dalmau J. Evidence for antibody-mediated pathogenesis in anti-NMDAR encephalitis associated with ovarian teratoma. *Acta Neuropathol*. 2009;118(6):737-743.
- Gong S, Zhou M, Shi G, et al. Absence of NMDA receptor antibodies in patients with ovarian teratoma without encephalitis. *Neurol Neuroimmunol Neuroinflamm*. 2017;4(3):e344.
- Armangue T, Spatola M, Vlagea A, et al. Frequency, symptoms, risk factors, and outcomes of autoimmune encephalitis after herpes simplex encephalitis: a prospective observational study and retrospective analysis. *Lancet Neurol*. 2018;17(9):760-772.
- Armangué T, Olivé-Cirera G, Martínez-Hernández E, et al. Neurologic complications in herpes simplex encephalitis: clinical, immunological and genetic studies. *Brain*. 2023;146(10):4306-4319.
- Small M, Treilleux I, Couillault C, et al. Genetic alterations and tumor immune attack in Yo paraneoplastic cerebellar degeneration. *Acta Neuropathol*. 2018;135(4):569-579.
- Tietz AK, Angstwurm K, Baumgartner T, et al. Genome-wide association study identifies 2 new loci associated with

- anti-NMDAR encephalitis. *Neurol Neuroimmunol Neuroinflamm.* 2021;8(6):e1085.
24. Kim TJ, Lee ST, Moon J, et al. Anti-LGI1 encephalitis is associated with unique HLA subtypes. *Ann Neurol.* 2017;81(2):183-192.
  25. van Sonderen A, Roelen DL, Stoop JA, et al. Anti-LGI1 encephalitis is strongly associated with HLA-DR7 and HLA-DRB4. *Ann Neurol.* 2017;81(2):193-198.
  26. Mueller SH, Färber A, Prüss H, et al. Genetic predisposition in anti-LGI1 and anti-NMDA receptor encephalitis. *Ann Neurol.* 2018;83(4):863-869.

## Supporting Information

Additional supporting information may be found online in the Supporting Information section at the end of the article.

**Figure S1.** Subject selection of patients with NMDARe and controls. From January 2014 to April 2020, 84 patients with NMDARe were recruited in our prospective autoimmune encephalitis cohort, and among them, 31 patients had ovarian teratomas. Excluding the absence of informed consent and surgery at an external hospital, 15 patients were finally selected who had available teratoma tissue. During the same period, non-encephalitic patients who had surgery due to teratoma were 508 in Seoul National University Hospital. Excluding 27 patients with immature teratoma, 481 patients were 1:2 age-matched with the chosen 15 patients with NMDARe. Eighteen patients who had available teratoma tissue were selected as the control group after a medical and pathology review. NMDAR, N-methyl-D-aspartic acid receptor.

**Figure S2.** The comparison of the mean VAF of SNVs/INDELs among peripheral blood of NMDARe, encephalitic teratoma, and control teratoma. There was a statistical difference in mean VAF between matched peripheral blood ( $n = 10$ ) and teratoma ( $n = 18$ ) from patients with NMDARe, but not between teratoma from patients with the encephalitis and control ( $n = 17$ ). INDEL, insertions and deletions; SNV, single-nucleotide variants; VAF, variant allele frequency.

**Figure S3.** The Manhattan plot of somatic mutations identified in encephalitic teratoma compared to their peripheral blood. The analysis was performed with the teratoma samples ( $n = 11$ ) which had matched peripheral blood samples. The red line indicates the significant threshold of  $5 \times 10^{-8}$ , and some variants above the line were annotated. However, the observed variations were not clinically significant, as the limited number of samples and the fact that no matched variants were found in the comparison between NMDARe-associated

and control teratomas (as shown in Fig. 1 and Table S6).

**Figure S4.** The mutational signatures of teratoma from patients with NMDARe and control using tumor-only data. The mutation signature analysis was performed to identify any underlying mutational processes that have shaped a particular set of genomic alterations in the NMDARe-associated teratomas compared to non-encephalitic control teratomas. The “S” followed by a number refers to a signature of single-base substitution mutations that are commonly found in cancer genomes and factors associated with DNA damage. The analysis revealed no significant difference in single-base substitution patterns between the two groups, indicating that no differences in mutational processes that have shaped the genomic landscape are present between the encephalitic and non-encephalitic teratomas. CT, control teratoma; ET, encephalitic teratoma.

**Figure S5.** The mutational signatures of somatic mutations identified in the NMDARe-associated teratoma matched with peripheral blood samples. The mutation signature analysis was performed with the NMDARe-associated teratoma samples ( $n = 11$ ) which had matched peripheral blood samples to identify any tumor-specific mutation pattern. The “SBS” followed by a number refers to a signature of single-base substitution mutations that are commonly found in cancer and factors associated with DNA damage. The analysis revealed no common single-base substitution pattern among the teratoma samples, suggesting the absence of specific mutational processes that have shaped the genomic landscape in NMDARe-associated teratomas.

**Table S1.** Results of sample DNA quality control. This table presents the results of DNA quality control for peripheral blood mononuclear cells and teratoma.

**Table S2.** Results of library DNA quality control. This table presents the results of library DNA quality control for peripheral blood mononuclear cells and teratoma.

**Table S3.** Teratoma sample analysis status of Patients with or without anti-NMDAR encephalitis. This table displays the analysis status of patients with or without anti-NMDAR encephalitis.

**Table S4.** Characteristics of Patients with anti-NMDAR encephalitis accompanied by ovarian teratoma. This table provides the characteristics of patients with anti-NMDAR encephalitis accompanied by ovarian teratoma.

**Table S5.** Characteristics of Patients with Ovarian teratoma Control group. This table displays the characteristics of patients with ovarian teratoma control group.

**Table S6.** Somatic mutation profiles of Patients with anti-NMDAR encephalitis and Control. This table presents the somatic mutation profiles of patients with anti-NMDAR encephalitis and control.